Charged Current Drell-Yan Production at N^{3}LO

Claude Duhr^a **Falko Dulat**^{b} **Bernhard Mistlberger**^{b}

^{a}*Theoretical Physics Department, CERN, CH-1211 Geneva 23, Switzerland.*

^{b}*SLAC National Accelerator Laboratory, 2575 Sand Hill Rd., Menlo Park, CA, 94025 USA*

E-mail: claude.duhr@cern.ch, falko.dulat@gmail.com, bernhard.mistlberger@gmail.com

ABSTRACT: We present the production cross section for a lepton-neutrino pair at the Large Hadron Collider computed at next-to-next-to-next-to leading order (N^{3}LO) in QCD perturbation theory. We compute the partonic coefficient functions of a virtual $W^\pm$ boson at this order. We then use these analytic functions to study the progression of the perturbative series in different observables. In particular, we investigate the impact of the newly obtained corrections on the inclusive production cross section of $W^\pm$ bosons, as well as on the ratios of the production cross sections for W^+, W^- and/or a virtual photon. Finally, we present N^{3}LO predictions for the charge asymmetry at the LHC.

Contents

1 Introduction

Cross sections for the production of leptons are among the ultimate precision observables measurable at the Large Hadron Collider (LHC) (see for example refs. [1–3]). As a consequence, they provide a unique window into the inner workings of collision processes at very high energies. The insights gained by studying them improve our understanding of the collider experiment and the fundamental mechanisms of scattering processes alike. To derive meaningful conclusions from such observations we must put our theoretical prediction for such scattering processes at the highest possible level. Here, we take one significant step in this direction and compute next-to-next-to-next-to leading order (N^{3}LO) predictions for the production cross section of a lepton-neutrino pair in QCD perturbation theory.

We focus on the charged current Drell-Yan [4] (CCDY) process, where a W boson is produced from the annihilation of two quarks with opposite isospin. In nature, the produced W boson decays within the blink of an eye, but the inclusive production probability of the bosons is easily related to the probability of producing a pair of fermions consisting of a neutrino and a charged lepton with invariant mass Q^2. These particles represent a stable final state and the charged lepton can be detected by the LHC experiments.

To derive theoretical predictions for the inclusive CCDY cross section we use the factorisation of hadronic cross sections into parton distribution functions (PDFs) and partonic cross sections. In order to achieve high precision predictions of the hadronic cross section, it is paramount to go beyond the Born approximation for the partonic cross section. In particular, we compute the desired partonic cross sections in the framework of perturbative QCD through N^{3}LO in the perturbative expansion in the strong coupling constant. The analytic formulæ for the partonic cross sections are some of the main results of this paper and are provided in electronic form together with its arXiv submission.

We then move on and study the impact of N^{3}LO corrections on various inclusive cross sections involving vector bosons. We focus on the progression of the perturbative series in QCD for some of the cleanest hadron collider observables. When combined with the

available N³LO results in the literature [5–14], our results are an important input to gauge the relevance and the impact of N³LO corrections on more differential observables, like fiducial cross sections. We also study cross section ratios for vector boson production, and observe a remarkable perturbative stability for these ratios.

This article is structured as follows: In Section 2 we briefly review the computation of the N³LO corrections to off-shell W production. In Section 3 we present our main result, namely phenomenological predictions for the W cross section at N³LO in QCD, and we discuss the main QCD uncertainties which affect the cross section at this order. In Section 4 we extend this analysis to ratios of vector boson cross sections and the charge asymmetry at the LHC. In Section 5 we draw our conclusions.

2 Setup of the computation

In this paper we compute higher-order corrections in the strong coupling constant to the charged-current Drell-Yan (CCDY) cross section, i.e., the inclusive cross section for the production of a lepton-neutrino pair of invariant mass Q^2 at a proton-collider with center-of-mass energy $\sqrt{S}$. Since we are only interested in QCD corrections, the lepton-neutrino pair can only be produced via the intermediate of an (off-shell) W boson. We can then factorise the production of the W boson from its subsequent decay and cast the cross section in the following form:

$$Q^2 \frac{d\sigma}{dQ^2}(p\,p \to W^\pm \to \ell^\pm \overset{(-)}{\nu}_\ell) = \frac{m_W^2}{12\pi^2\,v^2} \frac{Q^4}{(Q^2 - m_W^2)^2 + m_W^2\Gamma_W^2}\,\sigma_{W^\pm}(\tau)\,, \qquad (2.1)$$

where v is the vacuum expectation value and m_W and Γ_W are the mass and width of the W boson, and $\sigma_{W^\pm}$ denotes the inclusive cross section for the production of an off-shell $W^\pm$ boson with virtuality Q^2. Using QCD factorisation, this cross section can be written in the form

$$\sigma_{W^\pm}(\tau) = \tau\sigma_0 \sum_{i,j} f_i(\tau,\mu_F^2) \otimes \eta_{ij}^\pm(\tau,\mu_F^2,\mu_R^2) \otimes f_j(\tau,\mu_F^2)\,, \qquad (2.2)$$

where μ_F and μ_R denote the factorisation and renormalisation scales, and the $f_i(x,\mu_F^2)$ denote the parton density functions (PDFs) to find a parton species i with momentum fraction x inside the proton. Furthermore, $\tau = \frac{Q^2}{S}$ and $\eta_{ij}^\pm$ is the partonic coefficient for the production of an off-shell W boson from the parton species i and j. In the above equation we made use of convolutions defined by

$$f(x) \otimes g(x) = \int_x^1 \frac{dx'}{x'} f(x')g\left(\frac{x}{x'}\right)\,, \qquad (2.3)$$

and we introduced the normalisation factor

$$\sigma_0 = \frac{m_W^2 \pi}{n_c Q^2 v^2}\,, \qquad (2.4)$$

where n_c corresponds to the number of colours in QCD.

The partonic coefficients can be expanded into a perturbative series in the renormalised strong coupling constant $a_S = \alpha_S(\mu_R)/\pi$

$$\eta_{ij}^{\pm}(z) = \eta_{ij}^{\pm(0)}(z) + a_S\,\eta_{ij}^{\pm(1)}(z) + a_S^2\,\eta_{ij}^{\pm(2)}(z) + a_S^3\,\eta_{ij}^{\pm(3)}(z) + \dots . \qquad (2.5)$$

Above we have suppressed arguments of the functions indicating the dependence of the partonic coefficients on the perturbative scales. At leading order (LO) in α_S, it is only possible to produce a W boson from the annihilation of two (massless) quarks with opposite isospin:

$$\eta_{u_i \bar{d}_j}^{+(0)}(z) = |V_{u_i d_j}|^2\,\delta(1-z) \quad \text{and} \quad \eta_{d_i \bar{u}_j}^{-(0)}(z) = |V_{u_j d_i}|^2\,\delta(1-z)\,, \qquad (2.6)$$

where $V_{u_i d_j}$ denotes the Cabibbo-Kobayashi-Maskawa quark-mixing-matrix. Beyond LO [4], also other partonic channels open up. Perturbative corrections to the CCDY cross sections have been computed at next-to-leading order (NLO) in refs. [15–18] and at next-to-next-to-leading order (NNLO) in refs. [19–22]. The main result of this paper is to present for the first time phenomenological results for the production of an off-shell W boson at next-to-next-to-next-to-leading oder (N³LO) in perturbative QCD. Before we discuss our results in the next sections, we review in this section the main steps of the computation of the third-order corrections to the partonic coefficients.

The partonic coefficients are computable from Feynman diagrams, with $z = Q^2/\hat{s}$ and $\hat{s}$ the partonic center-of-mass energy. We have followed the same strategy as that for the computation of the inclusive cross section for Higgs boson production through gluon fusion and bottom-quark fusion [6, 8, 9, 23] and the inclusive Drell-Yan cross section [10]. In particular, the results were obtained using the framework of reverse unitarity [24–28] in order to compute all required interferences of real and virtual amplitudes contributing to the N³LO cross section. The required phase-space and loop integrals were carried out implicitly using integration-by-parts (IBP) identities [29–31], together with the method of differential equations [32–36]. This method allows one to represent the required integrated and interfered amplitudes in terms of linear combinations of *master integrals*. The purely virtual corrections are essentially identical to the case of the production of an off-shell photon, apart from the colour structure involving a cubic Casimir operator, which is absent here because of the non-diagonal flavour-structure of the charged-current interactions. The three-loop corrections for virtual photon production were first computed in refs. [37–43], and recomputed and confirmed in ref. [8]. Contributions with one real parton in the final state were considered in refs. [44–49] and the master integrals we used for our calculation were documented in refs. [44, 48]. Master integrals with two and three real partons were obtained for the purpose of ref. [6] and are based on results from refs. [23, 50–54].

We work in the $\overline{\text{MS}}$-scheme in conventional dimensional regularisation. The only interaction vertex that involves an axial coupling is the vertex involving the W boson. The non-diagonal flavour-structure of the charged-current interactions forces the W boson to be coupled twice to same connected fermion line in interference diagrams. As a consequence, vector and axial vector contributions to the hadronic cross section are identical and we only work with a vector current in the generation of our partonic coefficient functions. The ultraviolet (UV) counterterm for the strong coupling constant has been determined

through five loops in refs. [55–59]. Infrared (IR) divergences are absorbed into the definition of the PDFs using mass factorisation at N³LO [60–62]. The mass factorisation involves convoluting lower-order partonic cross sections with the three-loop splitting functions of refs. [63–65]. We have computed all the convolutions analytically in z-space using the POLYLOGTOOLS package [66]. After combining our interfered matrix elements with the UV and PDF-IR counterterms we send the dimensional regulator to zero and obtain our final results. Our partonic coefficients are expressed in terms of the iterated integrals in z defined in ref. [6]. While many of these iterated integrals can be expressed in terms of harmonic or multiple polylogarithms [67, 68], some integration kernels involve elliptic integrals. It is currently unknown how to express them in terms of known functions. In ref. [6] it was shown how to obtain fast converging series representations which allow one to achieve a relative numerical precision of (at least) 10^{-10} in the whole range $z \in [0, 1]$ for all partonic coefficients.

The analytic results for the partonic coefficients are provided as ancillary material with the arXiv submission. Besides the explicit analytic cancellation of the UV and IR poles, we have performed various checks to establish the correctness of our computation. First, we have checked that all logarithmic terms in the renormalisation and factorisation scales produced from the cancellation of the UV and IR poles satisfy the Dokshitzer-Gribov-Lipatov-Altarelli-Parisi (DGLAP) evolution equation [69–71]. Second, the limit of soft-gluon emission, which corresponds to $z \to 1$, is independent of the form of the hard interaction process and only depends on the quantum numbers of the initial-state partons. Hence, the soft-virtual cross sections must be identical to the ones for neutral-current Drell-Yan production (again, apart from the contribution from the cubic Casimir operator). We have reproduced the soft-virtual N³LO cross section of refs. [51, 72–76], and also the physical kernel constraints of refs. [77–79] for the next-to-soft term of the quark-initiated cross section. The high-energy limit of the cross section, which corresponds to $z \to 0$, must also be identical between charged- and neutral-current production, and we have checked that our partonic cross sections have the expected behaviour in the high-energy limit [80, 81]. Finally, we have checked that we reproduce the numerical results for the ratios of the inclusive W^+ and W^- cross sections up to NNLO given in ref. [82].

3 W-production at N³LO

In this section we discuss our phenomenological results for inclusive (off-shell) W-production at N³LO. All results were obtained in a theory with $N_f = 5$ massless quark flavours (two up-type and three down-type flavours). The values of the mass and the width of the W boson are $m_W = 80.379\,\text{GeV}$ and $\Gamma_W = 2.085\,\text{GeV}$, and the vacuum expectation value is $v = 246.221\,\text{GeV}$. The elements of the CKM matrix relevant to our computation are [83]:

$$|V_{ud}| = 0.97446\,, \qquad |V_{us}| = 0.22452\,, \qquad |V_{ub}| = 0.00365\,,$$
$$|V_{cd}| = 0.22438\,, \qquad |V_{cs}| = 0.97359\,, \qquad |V_{cb}| = 0.04214\,. \tag{3.1}$$

Note that only the absolute values of the entries of the CKM matrix enter our computation. In our phenomenological results the top quark is absent, which is equivalent to having $V_{td_i} =$

0 and only considering $N_f = 5$ massless degrees of freedom in loops. This approximation is motivated because off-diagonal CKM matrix elements are small and diagrams without a coupling of the top quark to the electroweak gauge boson decouple in the limit of infinite top quark mass. Corrections to this approximation, which are expected to be very small, can be computed separately and are beyond the scope of this article. The strong coupling constant is evolved to the renormalisation scale μ_R using the four-loop QCD beta function in the $\overline{\text{MS}}$-scheme assuming $N_f = 5$ active, massless quark flavours. Unless stated otherwise, all results are obtained for a proton-proton collider with $\sqrt{S} = 13\,\text{TeV}$ using the zeroth member of the combined `PDF4LHC15_nnlo_mc` set [84].
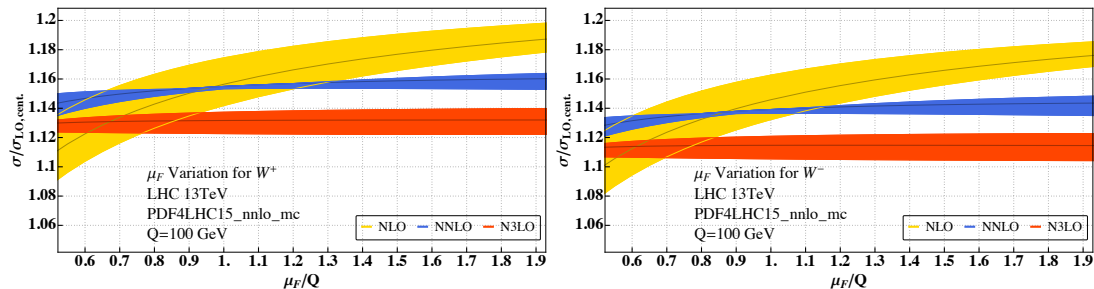

Figure 1: The cross sections for producing a W^+ (left) or W^- (right) for $\mu_R = Q = 100\,\text{GeV}$ as a function of the factorisation scale μ_F. The bands are obtained by varying μ_R by a factor of 2 up and down. The cross sections are normalised to the leading order cross section evaluated at $\mu_F = \mu_R = Q$.
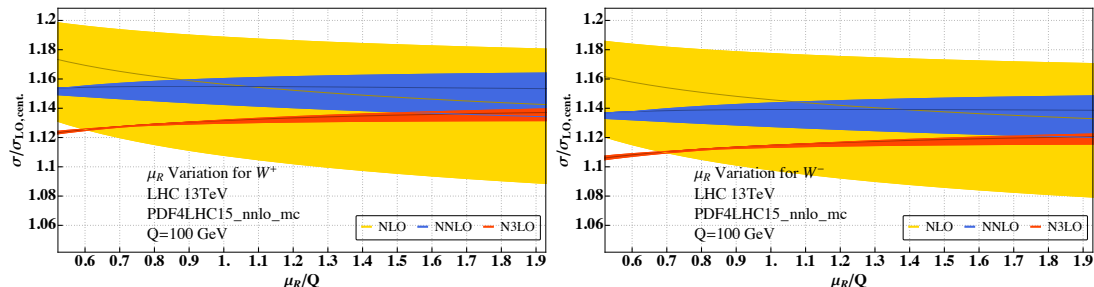

Figure 2: The cross sections for producing a W^+ (left) or W^- (right) for $\mu_F = Q = 100\,\text{GeV}$ as a function of the renormalisation scale μ_R. The bands are obtained by varying μ_F by a factor of 2 up and down. The cross sections are normalised to the leading order cross section evaluated at $\mu_F = \mu_R = Q$.

Figures 1 and 2 show the dependence of the fixed-order cross sections on the factorisation scale μ_F and renormalisation scale μ_R, which are introduced by the truncation of the perturbative series. We show the variation of the cross section for $Q = 100\,\text{GeV}$ on one of the two scales with the other held fixed at Q. We observe that the dependence on the perturbative scales is substantially reduced as we increase the perturbative order. The dependence on the scales looks very similar to the case of the N^{3}LO cross section for the neutral-current process studied in ref. [10]. We notice, that the dependence of the cross

section on the renormalisation scale is slightly larger than on the factorisation scale.

Next, in order to quantify the size of the N^{3}LO corrections, we investigate the K-factors:

$$K_{W^\pm}^{N^3LO}(Q) = \frac{\sigma_{W^\pm}^{(3)}(\mu_F = \mu_R = Q)}{\sigma_{W^\pm}^{(2)}(\mu_F = \mu_R = Q)},$$
$$\delta(\text{scale}) = \frac{\delta_{\text{scale}}(\sigma_{W^\pm}^{(3)})}{\sigma_{W^\pm}^{(3)}(\mu_F = \mu_R = Q)}, \tag{3.2}$$

where $\sigma_{W^\pm}^{(n)}(\mu_F = \mu_R = Q)$ is the hadronic cross section including perturbative corrections up to n^{th} order evaluated for $\mu_F = \mu_R = Q$ and $\delta_{\text{scale}}(\sigma_{W^\pm}^{(n)})$ is the absolute uncertainty on the cross section from varying μ_F and μ_R independently by a factor of two up and down around the central scale $\mu^{\text{cent}} = Q$ such that $\frac{1}{2} \leq \frac{\mu_F}{\mu_R} \leq 2$ (7-point variation).

Q/GeV	$K_{W^+}^{N^3LO}$	$K_{W^-}^{N^3LO}$	$K_{\gamma^*}^{N^3LO}$
30	$0.953^{+2.5\%}_{-1.7\%}$	$0.950^{+2.6\%}_{-1.6\%}$	$0.952^{+2.5\%}_{-1.5\%}$
50	$0.966^{+1.5\%}_{-1.2\%}$	$0.964^{+1.6\%}_{-1.2\%}$	$0.966^{+1.6\%}_{-1.1\%}$
70	$0.974^{+1.1\%}_{-1.0\%}$	$0.972^{+1.2\%}_{-0.9\%}$	$0.973^{+1.1\%}_{-0.9\%}$
80.379	$0.976^{+1.0\%}_{-0.9\%}$	$0.975^{+1.0\%}_{-0.9\%}$	$0.976^{+1.0\%}_{-0.8\%}$
90	$0.978^{+0.9\%}_{-0.8\%}$	$0.977^{+0.9\%}_{-0.8\%}$	$0.978^{+0.9\%}_{-0.7\%}$
110	$0.981^{+0.7\%}_{-0.7\%}$	$0.980^{+0.8\%}_{-0.7\%}$	$0.981^{+0.7\%}_{-0.6\%}$
130	$0.984^{+0.6\%}_{-0.6\%}$	$0.982^{+0.6\%}_{-0.6\%}$	$0.983^{+0.6\%}_{-0.6\%}$
150	$0.985^{+0.5\%}_{-0.5\%}$	$0.984^{+0.6\%}_{-0.5\%}$	$0.985^{+0.5\%}_{-0.5\%}$
500	$0.997^{+0.2\%}_{-0.1\%}$	$0.996^{+0.2\%}_{-0.1\%}$	$0.996^{+0.2\%}_{-0.1\%}$
800	$0.999^{+0.09\%}_{-0.05\%}$	$0.999^{+0.1\%}_{-0.05\%}$	$0.999^{+0.09\%}_{-0.04\%}$

Table 1: The QCD K-factor at N^{3}LO for charged-current and neutral-current Drell-Yan production. All central values and uncertainties are computed according to eq. (3.2). The results for neutral-current Drell-Yan production are taken from ref. [10].

Table 1 shows the results for the K-factors for both charged- and neutral-current Drell-Yan production for various values of Q (the results for the neutral-current process are taken from ref. [10]). We observe that the K-factor reaches up to 5% for small values of Q, and the impact of the N^{3}LO corrections gets smaller as Q increases. Moreover, we find that the K-factors at N^{3}LO are identical between the charged- and neutral-current processes, confirming and extending results at lower orders, and hinting towards a universality of QCD corrections to vector-boson production in proton collisions.

Figure 3 shows the values of the cross section normalised to the N^{3}LO cross section as a function of the virtuality Q. The uncertainty bands are obtained by varying the renormalisation and factorisation scales independently up and down as described above around the central scale $\mu^{\text{cent}} = Q$. We observe that for $Q \gtrsim 50\,\text{GeV}$ the scale-variation bands at NNLO and N^{3}LO do not overlap. A similar feature was already observed for
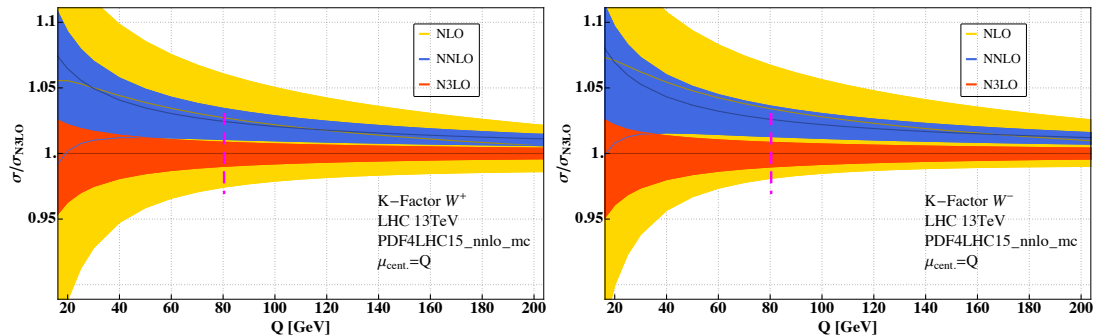
Figure 3: The cross sections for producing a W^+ (left) or W^- (right) as a function of the virtuality Q normalised to the N³LO prediction. The uncertainty bands are obtained by varying μ_F and μ_R around the central scale $\mu^{\mathrm{cent}} = Q$. The dashed magenta line indicates the physical W boson mass, $Q = m_W$.

virtual photon production in ref. [10], hinting once more towards a universality of the QCD corrections to these processes.
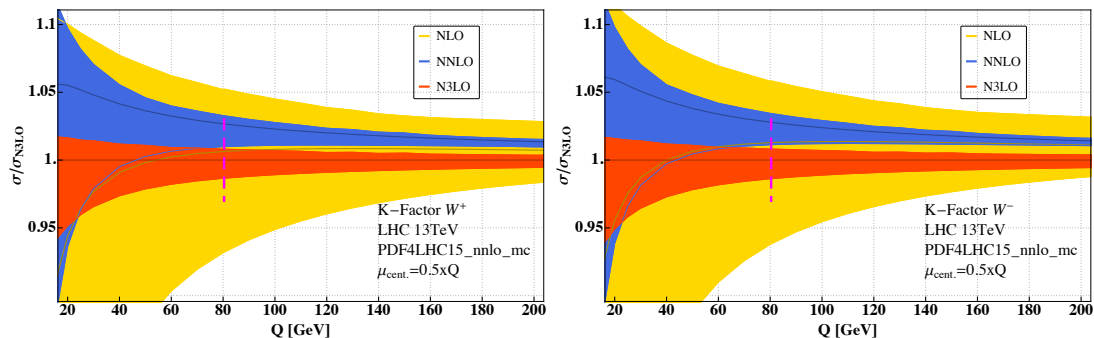

Figure 4: The cross sections for producing a W^+ (left) or W^- (right) as a function of the virtuality Q. The uncertainty bands are obtained by varying μ_F and μ_R around the central scale $\mu^{\mathrm{cent}} = Q/2$. The dashed magenta line indicates the physical W boson mass, $Q = m_W$.

Figure 4 shows the scale variation of the cross section with a different choice for the central scale, $\mu^{\mathrm{cent}} = Q/2$. It is known that for Higgs production a smaller choice of the factorisation scale leads to an improved convergence pattern and the bands from scale variations are strictly contained in one another. We observe here that the two scale choices share the same qualitative features.

The fact that the scale variation bands do not overlap puts some doubt on whether it gives a reliable estimate of the missing higher orders in perturbation theory, or whether other approaches should be explored (cf., e.g., refs. [85, 86]). In ref. [10] it was noted that for virtual photon production there is a particularly large cancellation between different initial state configurations. We observe here the same in the case of W boson production. This cancellation may contribute to the particularly small NNLO corrections and scale variation bands, and it may be a consequence of the somewhat arbitrary split of the content

of the proton into quarks and gluons. If these cancellations play a role in the observed perturbative convergence pattern, then it implies that one cannot decouple the study of the perturbative convergence from the structure of the proton encoded in the PDFs. We will return to this point below, when we discuss the effect of PDFs on our cross section predictions.
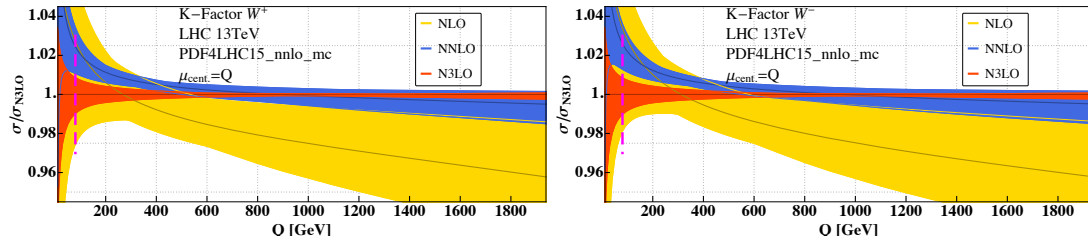

Figure 5: The cross sections for producing a W^+ (left) or W^- (right) as a function of the virtuality Q. The uncertainty bands are obtained by varying μ_F and μ_R around the central scale $\mu^{\mathrm{cent}} = Q$. The dashed magenta line indicates the physical W boson mass, $Q = m_W$.

Figure 5 shows the production cross section for an off-shell W boson normalised to the prediction at N³LO for a larger range of virtualities ($Q \le 2\,\mathrm{TeV}$). We see that for larger values of the virtuality ($Q > 550\,\mathrm{GeV}$) the bands derived from scale variation at NNLO and N³LO start to overlap. We also observe a more typical shrinking of the scale variation bands as well as a small correction at N³LO.
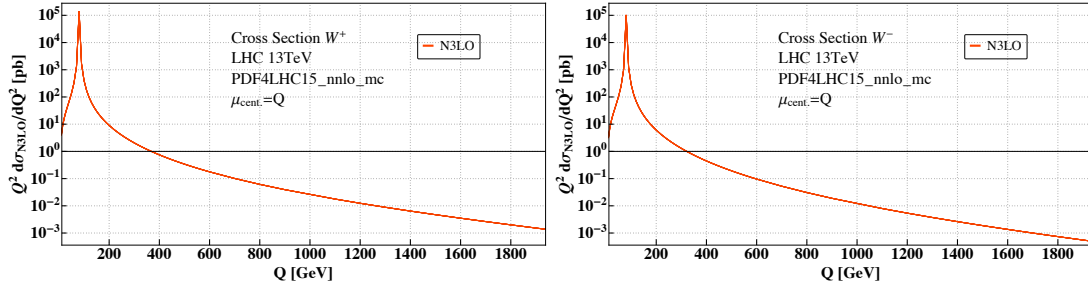

Figure 6: The cross sections for producing a lepton-neutrino pair via an off-shell W boson as a function of the invariant mass of the final state, or equivalently the virtuality of the W boson, cf. eq. (2.1).

Figure 6 shows the nominal production cross section of a lepton-neutrino pair at the LHC at 13 TeV centre of mass energy, as defined in eq. (2.1).

Figure 7 shows the variation of K-factors as a function of the energy of the hadron collider for $Q = 100$ GeV. The orange, blue and red bands correspond to predictions with the perturbative cross section truncated at NLO, NNLO and N³LO, and the size of the band is obtained by performing a 7-point variation of (μ_F, μ_R) around the central scale $\mu^{\mathrm{cent}} = Q$. We observe that the NLO, NNLO and N³LO K-factors are relatively independent of the centre of mass energy. Furthermore, we see that the bands due to scale
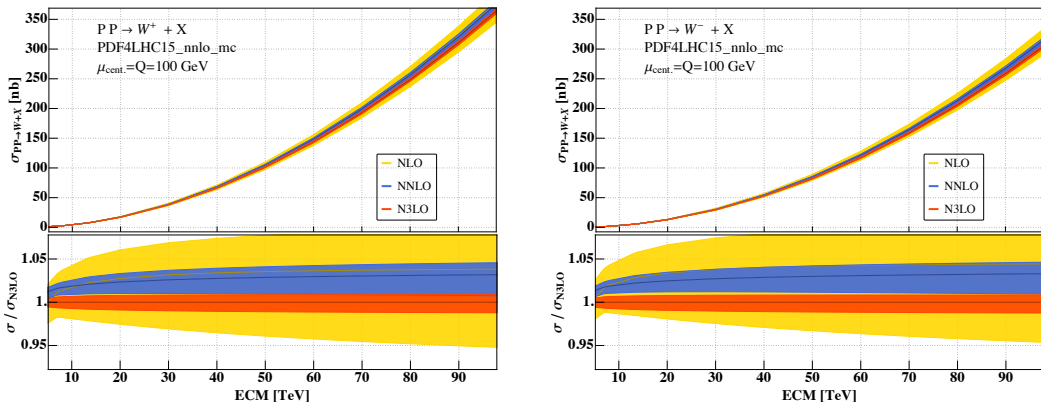
Figure 7: The cross sections for producing a W^+ (left) or W^- (right) as a function of the hadronic centre of mass energy for $Q = 100$ GeV. The uncertainty bands are obtained by varying μ_F and μ_R around the central scale $\mu^{\text{cent}} = Q$ (see text for details).

variation at NNLO and N³LO do not overlap for a large range of center of mass energies. However, the gap is narrowed at the extreme end of the range of energies considered here.

Parton distribution functions are extracted from a large set of measurements and are consequently subject to an uncertainty related to the input as well as to the methodology used to extract the PDFs. Here, we follow the prescription of ref. [84] for the computation of PDF uncertainties $\delta(\text{PDF})$ using the Monte Carlo method. Furthermore, also the strong coupling constant is an input parameter for our computation. The PDF set `PDF4LHC15_nnlo_mc` uses $\alpha_S = 0.118$ as a central value and two additional PDF sets are available that allow for the correlated variation of the strong coupling constant in the partonic cross section and the PDF sets to $\alpha_S^{\text{up}} = 0.1195$ and $\alpha_S^{\text{down}} = 0.1165$. This sets allow us to deduce an uncertainty $\delta(\alpha_S)$ on our cross section following the prescription of ref. [84]. We combine the PDF and strong coupling constant uncertainties in quadrature to give

$$\delta(\text{PDF} + \alpha_S) = \sqrt{\delta(\text{PDF})^2 + \delta(\alpha_S)^2} \,. \tag{3.3}$$

In our computation we use NNLO-PDFs, because currently there is no available PDF set extracted from data with N³LO accuracy. It is tantalising to speculate if the observed convergence pattern is related to the mismatch in perturbative order used for the PDFs and the partonic cross section. We estimate the potential impact of this mismatch on our cross section predictions using a prescription introduced in ref. [5] that studies the variation of the NNLO cross section as NNLO- or NLO-PDFs are used. This defines the PDF theory uncertainty

$$\delta(\text{PDF-TH}) = \frac{1}{2} \left| \frac{\sigma_{W^\pm}^{(2), \text{ NNLO-PDFs}} - \sigma_{W^\pm}^{(2), \text{ NLO-PDFs}}}{\sigma_{W^\pm}^{(2), \text{ NNLO-PDFs}}} \right| \,. \tag{3.4}$$

Here, the factor $\frac{1}{2}$ is introduced as it is expected that this effect becomes smaller at N³LO compared to NNLO.
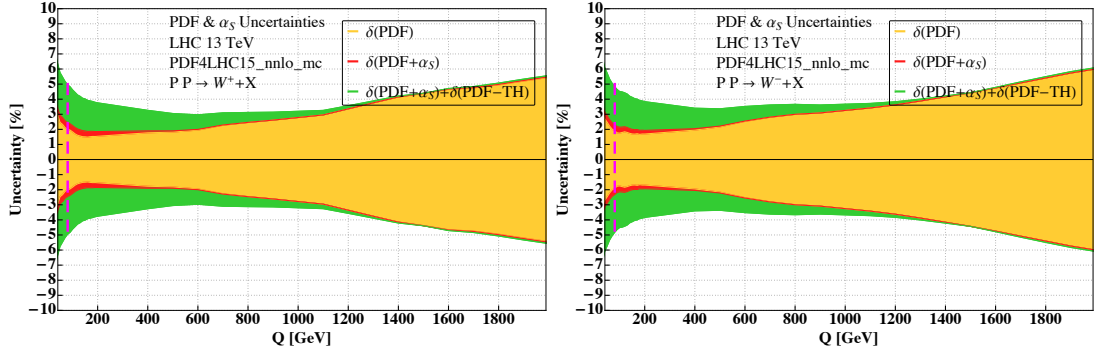
Figure 8: Sources of uncertainty as a function of Q for the W^+ (left) and W^- (right) K-factors. δ(PDF), δ(PDF+α_S) and the sum of δ(PDF+α_S) and δ(PDF-TH) are shown in orange, red and green respectively. The dashed magenta line indicates the physical W boson mass, $Q = m_W$.

Figure 8 displays the uncertainties δ(PDF), δ(PDF+α_S) and δ(PDF-TH) as a function of Q in orange, red and green respectively. In particular, the green band indicates the sum δ(PDF+α_S)+δ(PDF-TH). Our findings for δ(PDF) are compatible with the results of for example refs. [84, 87] where PDF effects on W boson cross sections were discussed in more detail. We observe that the estimate for δ(PDF-TH) plays a significant role especially for low values of Q. The traditional PDF uncertainty has a stronger impact for larger values of Q. Overall, we observe that the relative size of δ(PDF) and δ(PDF-TH) is large in comparison to the effect of varying the scales. We conclude that future improvements in the precision of the prediction of this observable will have to tackle the problem of the uncertainties discussed here. In particular, we emphasize that the relatively large size of δ(PDF-TH) can potentially have a substantial impact on the central value of the N^{3}LO correction, especially for smaller values of Q. As discussed above, there are large intricate cancellations between different initial state channels at N^{3}LO. This implies that a small relative change of quark vs. gluon parton densities at N^{3}LO may have an enhanced effect on the perturbative cross section as a result. We can only wonder if the usage of true N^{3}LO parton densities could lead to N^{3}LO predictions that are fully contained in the scale variation band of the previous order. However, in the absence of N^{3}LO PDFs, we can only stress the importance estimating an uncertainty due to the missing N^{3}LO PDFs and suggest δ(PDF-TH) as a possible estimator.

4 Predictions for cross section ratios

In the previous section, we have seen that the conventional variation of the perturbative scales by a factor of 2 does not give a reliable estimate of the size of the missing higher orders. This motivates us to study the ratios of cross sections for the production of gauge bosons with virtuality Q:

$$R_{XY}(Q) = \frac{\sigma_X(Q)}{\sigma_Y(Q)}, \qquad X, Y \in \{W^\pm, \gamma^*\}. \tag{4.1}$$

Indeed, since the charged- and neutral-current Drell-Yan processes show very similar K-factors and dependences on the perturbative scales, it is conceivable that some of the uncertainties (e.g., PDF effects) cancel in the ratio, and the ratios may exhibit an enhanced perturbative stability. In the remainder of this section we analyse and compare different prescriptions to estimate the missing higher orders in the perturbative expansion of the cross section ratios for $\sqrt{S} = 13\,\text{TeV}$. We focus here on the following prescriptions:

- **Prescription A:** We take the ratio of the perturbative expansion of the numerator and the denominator computed at a given order in perturbation theory. We choose the renormalisation and factorisation scales in the numerator and denominator in a correlated way, i.e., we always choose the same values for the scales in both the numerator and the denominator.

- **Prescription B:** Similar to Prescription A, but we do not correlate the renormalisation and factorisation scales between the numerator and the denominator. In other words, we perform independently a 7-point variation of the scales in the numerator and the denominator, and we take the envelope of the values obtained.

- **Prescription A′:** We choose the scales in a correlated way, but we expand the ratio in perturbation theory and only retain terms through a given order in the strong coupling.

- **Prescription B′:** Similar to Prescription A′, but we choose the scales in an uncorrelated way.

- **Prescription C:** We take the relative size of the last considered order compared to the previous one as an estimator of the perturbative uncertainty:

$$\delta(\text{pert.}) = \pm \left| 1 - \frac{R_{XY}^{(n)}(Q)}{R_{XY}^{(n-1)}(Q)} \right| \times 100\% \,. \tag{4.2}$$

The superscript n on $R_{XY}^{(n)}(Q)$ indicates the order at which we truncate the perturbative expansion. The values of $\mu_F = \mu_R = \mu^{\text{cent}}$ are chosen in a correlated way in the numerator and the denominator of R_{XY}. This estimator is based on the expectation that in a well-behaved perturbative expansion the subleading terms should be smaller than the last known correction. By construction, it leads to an estimate of the missing higher orders that is symmetric around the central value.

Note that Prescriptions A, A′, B and B′ are fully equivalent to all orders in perturbation theory. The truncation of the perturbative series can, however, introduce differences in the results obtained from these four prescriptions, especially at low orders in perturbation theory. For example, the bands obtained by varying the scales will always be larger if the scales are varied in an uncorrelated way, because in that case the size of the band is obtained by taking the envelope of a strictly larger set of values.

Table 2 shows the prediction for $R_{W^+W^-}$ for $Q = m_W$ computed at the first few orders in perturbation theory. First, we see that the central value is extremely stable in

μ^{cent}	NLO		NNLO		N^{3}LO	
	m_W	$m_W/2$	m_W	$m_W/2$	m_W	$m_W/2$
A	$1.342^{+0.10\%}_{-0.08\%}$	$1.342^{+0.07\%}_{-0.05\%}$	$1.348^{+0.12\%}_{-0.10\%}$	$1.349^{+0.15\%}_{-0.11\%}$	$1.350^{+0.05\%}_{-0.06\%}$	$1.350^{+0.04\%}_{-0.05\%}$
A$'$	$1.343^{+0.13\%}_{-0.16\%}$	$1.344^{+0.10\%}_{-0.21\%}$	$1.349^{+0.13\%}_{-0.09\%}$	$1.351^{+0.33\%}_{-0.13\%}$	$1.350^{+0.02\%}_{-0.03\%}$	$1.350^{+0.01\%}_{-0.09\%}$
B	$1.342^{+8.82\%}_{-8.08\%}$	$1.342^{+12.9\%}_{-11.4\%}$	$1.348^{+2.26\%}_{-2.31\%}$	$1.349^{+2.24\%}_{-2.27\%}$	$1.350^{+2.21\%}_{-2.14\%}$	$1.350^{+2.21\%}_{-2.14\%}$
B$'$	$1.343^{+5.28\%}_{-7.40\%}$	$1.344^{+8.09\%}_{-8.97\%}$	$1.349^{+1.85\%}_{-2.63\%}$	$1.351^{+2.21\%}_{-2.24\%}$	$1.350^{+2.60\%}_{-2.25\%}$	$1.350^{+4.65\%}_{-2.70\%}$
C	$1.342^{+0.99\%}_{-0.99\%}$	$1.342^{+0.58\%}_{-0.58\%}$	$1.349^{+0.52\%}_{-0.52\%}$	$1.349^{+0.53\%}_{-0.53\%}$	$1.350^{+0.15\%}_{-0.15\%}$	$1.350^{+0.11\%}_{-0.11\%}$

Table 2: The ratio $R_{W^+W^-}$ for $Q = m_W$ computed for different values of μ^{cent} and with the different prescriptions mentioned in the text.

perturbation theory, changing only at the permille level as we go from NNLO to N^{3}LO. The central value is pretty much independent of the choice of the central scale μ^{cent} and whether the ratio is expanded in perturbation theory or not (primed vs. unprimed prescriptions). While in general the different prescriptions lead to vastly different estimates of the missing higher orders, the predictions are similar between the primed vs. unprimed prescriptions, especially as we increase the perturbative order. This is to be expected: If the perturbative order is increased, the differences stemming from expanding or not the denominator of the ratio should decrease, which is indeed what we observe. We therefore only discuss the unprimed prescriptions from now on. Second, we observe that Prescription B leads to an estimate that is more than an order of magnitude larger than for Prescriptions A and C. In particular, this makes one wonder if correlated scales (Prescription A & C) tend to underestimate the size of the missing higher-order terms beyond N^{3}LO. We believe that results obtained from uncorrelated scales (Prescription B) lead to estimates that are too conservative. Indeed, since the central value of the ratio only receives permille-level corrections from NNLO to N^{3}LO and exhibits extremely good perturbative stability, one expects higher-order corrections to be at the sub-permille level, which is indeed the size of the band obtained by varying the scales in a correlated way (Prescription A & C). It would be unreasonable to expect that the missing higher-order corrections shift the central value by 1% or even more, which is the size of the bands obtained from the uncorrelated prescription (Prescription B). A correlated prescription is also motivated by the fact that the neutral- and charged-current processes are expected to receive very similar QCD corrections, a fact which is corroborated by the results from the previous section. Finally, we observe that Prescription C leads to an estimate that is always slightly larger (by a factor ~ 3 for $Q = m_W$) than the one obtained from Prescription A at N^{3}LO. We have observed that the size of the higher-order terms estimated from Prescription A always encompasses the next order in perturbation theory. In order words, Prescription A appears to account for the effect of missing higher orders even though it estimates relatively small residual uncertainties for the point $Q = m_W$. Below we study ratios of cross sections as a function of a range of different values of Q allowing us to comment on Prescription A in more detail.
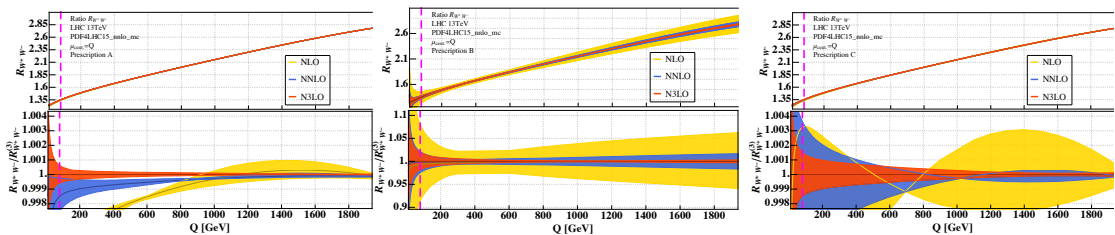
Figure 9: The upper panels show the ratio $R_{W^+W^-}$ (left) with bands computed with Prescription A (left), Prescription B (middle) and Prescription C (right). The lower panels show the same normalised to the value of the ratio computed at N³LO. The dashed magenta line indicates the physical W boson mass, $Q = m_W$.

Figure 9 shows the ratio $R_{W^+W^-}$ as a function of the virtuality Q. The bands were created using Prescription A (left), B (middle) and C (right). Just like for on-shell production, we observe that correlated and uncorrelated scales lead to vastly different estimates for the size of the bands. In particular, Prescription B gives an extremely conservative estimate of the bands over the whole range of Q considered. Unlike for on-shell production, the bands obtained from Prescription A do not overlap for $Q > 200\,\mathrm{GeV}$, which indicates that Prescription A does not correctly capture the size of higher-order corrections in this range of virtualities. In general, this calls into question whether correlated scale variations should be used as an uncertainty estimator for ratios of cross sections with very similar K-factors. Instead, Prescription C seems to give the most reliable estimator of the size of the residual perturbative corrections for ratios of cross sections over the whole range of virtualities considered.
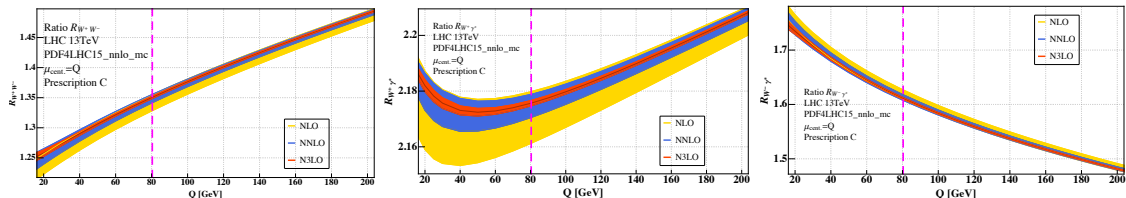

Figure 10: The ratios $R_{W^+W^-}$ (left), $R_{W^+\gamma^*}$ (middle) and $R_{W^+\gamma^*}$ (right) as a function of the virtuablity Q. The uncertainty bands are obtained with Prescription C for the central scale $\mu^{\mathrm{cent}} = Q$. The dashed magenta line indicates the physical W boson mass, $Q = m_W$.

In fig. 10 we extend our analysis from $R_{W^+W^-}$ (left) to $R_{W^+\gamma^*}$ (middle) and $R_{W^+\gamma^*}$ (right). In all cases the bands are estimated using Prescription C. Similar to our discussion in the previous paragraph, we find that Prescription C delivers reliable estimates also for the latter two ratios. In all cases we find that the residual perturbative uncertainty is very small, making ratios of production cross sections of electroweak gauge bosons very stable under perturbative corrections, and therefore ideal precision observables.

While Prescription C seems to give reliable estimates for all cross section ratios considered over a wide range of kinematics, we have to point out that Prescription C has the obvious shortcoming that it gives a vanishing result whenever two consecutive perturbative

orders give identical numerical predictions. The same fact leads to rather unconventional shapes of the uncertainty band as a function of Q. Consequently, prescription C on its own would not serve as a good estimator of perturbative uncertainties. For example, it predicts vanishing perturbative uncertainty of $R_{W^+W^-}$ at NLO around $Q = 700$ GeV, which is clearly unreliable. In order to estimate perturbative uncertainties we therefore suggest that multiple different perspectives and estimators should be considered, in order to test the quality of the estimates obtained. For the future, it would be interesting to investigate other prescriptions to estimate the impact of missing perturbative orders, including prescriptions based on statistical methods [85, 86]. A more detailed study of these effects, however, would go beyond the scope of this paper.

We finish by presenting results for an observable which is closely related to the ratio $R_{W^+W^-}$. The lepton-charge asymmetry is defined as:

$$A_W(Q) = \frac{\sigma_{W^+}(Q) - \sigma_{W^-}(Q)}{\sigma_{W^+}(Q) + \sigma_{W^-}(Q)} = \frac{R_{W^+W^-}(Q) - 1}{R_{W^+W^-}(Q) + 1}. \tag{4.3}$$
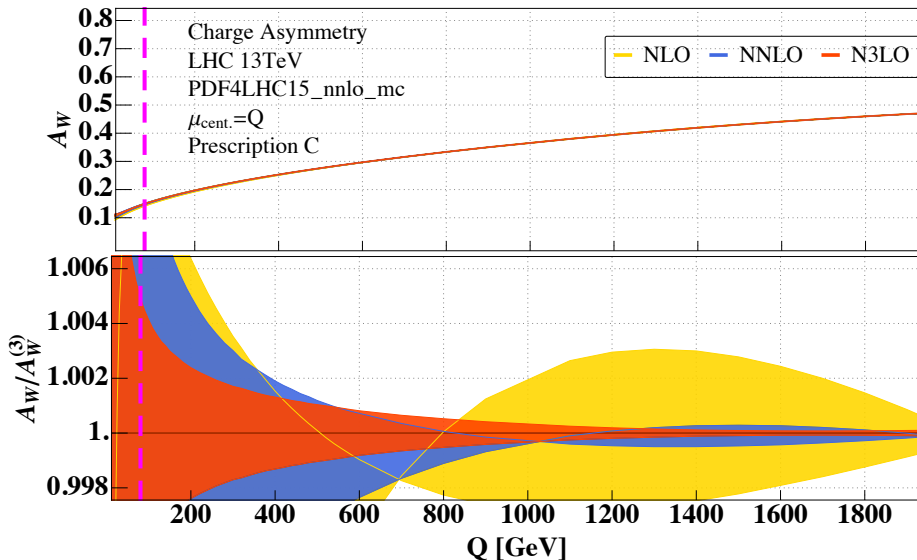

Figure 11: The lepton-charge asymmetry A_W as a function of the virtuality Q. The uncertainty bands are obtained with Prescription C. The dashed magenta line indicates the physical W boson mass, $Q = m_W$.

Figure 11 shows our predictions for the lepton-charge asymmetry as a function of Q at different orders in perturbation theory. All uncertainty bands are obtained from Prescription C. Just like the cross section ratios studied earlier, we observe a good perturbative stability and a very small residual dependence on the perturbative scales at N^{3}LO. In particular, for $Q = m_W$, we find

$$
\begin{aligned}
A_W^{(2)}(m_W) &= 0.148^{+0.41\%}_{-0.34\%}, \\
A_W^{(3)}(m_W) &= 0.149^{+0.15\%}_{-0.19\%}.
\end{aligned}
\tag{4.4}
$$

So far we have only discussed the uncertainties on cross section ratios from the truncation of perturbative orders. We therefore conclude by commenting on uncertainties on ratios related to PDFs, similar to those considered in Section 3. Just like in the case of the perturbative uncertainty, a choice has to be made whether or not to treat PDF and strong coupling constant variation as correlated in numerator and denominator of the ratio. The fact that PDFs and α_S are universal quantities suggests indeed a correlated treatment. In this case, ratios of cross sections could provide a remarkable tool to reduce some of the largest theoretical uncertainties afflicting the observables in question. However, in neutral current and charged current DY production cross section different combinations of parton distribution functions play a dominant role. This could indeed spoil a correlated treatment of PDF uncertainties and should be studied in more detail.

5 Conclusion

In this paper we have computed for the first time the N^3LO corrections to the inclusive production cross section of a lepton-neutrino pair at a proton-proton collider in QCD perturbation theory. One of the main results of this article are analytic formulæ for the partonic coefficient functions for this cross section, which we make available as ancillary material with the arXiv submission of this paper.

We have studied the phenomenological impact of our results by providing numerical results for (off-shell) W-production at the LHC. All our results are differential in the virtuality of the W boson, or equivalently in the invariant mass of the lepton-neutrino pair. We find that the N^3LO corrections are at the level of a few percent and they stabilise the perturbative progression of the series. We have also studied ratios of cross sections for W^+, W^- and γ^*, as well as the charge asymmetry at the LHC, i.e., the amount of produced W^+ bosons relative to the amount W^- bosons. We find that these ratios feature a remarkable perturbative stability and that they can be predicted with very high precision. For the future, it would be interesting to study, in addition to the QCD corrections discussed here, how the inclusive production probability of weak bosons is impacted by electroweak and QED corrections, for example the electroweak and mixed QCD-electroweak corrections to Drell-Yan processes of refs. [88–98]. While such a study is beyond the scope of this article, we would like to stress their importance here.

Combined with the results for virtual photon production of ref. [10], our results have also allowed us to investigate the progression of the perturbative series through N^3LO in QCD for one of the simplest classes of hadron collider observables, namely fully inclusive vector boson production cross sections. Understanding the perturbative convergence of this class of processes is an important proxy to understand the precision that can be reached more generally for LHC observables at this order in perturbation theory. Here we summarise our main observations and conclusions, and the possible implications for a precision physics program at the LHC. First, we observe in all cases that the N^3LO corrections shift the central value of the predictions by a few percent. This implies that, very likely, also for more differential observables percent-level precision can only be achieved after the inclusion of N^3LO corrections. It would be interesting to develop and extend

techniques to perform differential calculations at N^{3}LO (see, e.g., refs. [12–14, 99–101] for first steps in this direction). Second, we observe that the uncertainties related to PDFs generically dominate over the residual perturbative uncertainty at N^{3}LO. This motivates to push for determining PDFs at this order in perturbation theory, by extracting them from experimental measurements confronted to theory calculations performed at the same order, and to evolve them using the (yet unknown) DGLAP evolution kernels at N^{4}LO. Finally, we observe that the conventional method to estimate the missing higher-order terms by varying the factorisation and renormalisation scales by a factor of two around a hard scale does not give reliable results at N^{3}LO. This calls for an improved method to estimate the missing higher-order terms, e.g., by studying the progression of the perturbative series as done here, or by considering statistically-motivated techniques such as those of refs. [85, 86]. However, we have also observed that the determination of the residual perturbative uncertainty may not be completely decoupled from the study of PDF effects: Indeed, we observe substantial cancellations between different partonic channels. It is tantalising to speculate if these cancellations are responsible for the non-overlapping scale variation bands at N^{3}LO, and if they persist once a complete set of N^{3}LO PDFs is available. A detailed study of these effects, however, goes beyond the scope of this paper and is left for future work.

Acknowledgements

References

[1] **ATLAS** Collaboration, G. Aad *et al.*, *Measurement of $W^\pm$ and Z-boson production cross sections in pp collisions at $\sqrt{s} = 13$ TeV with the ATLAS detector*, Phys. Lett. **B759** (2016) 601–621, [1603.09222].

[2] **CMS** Collaboration, C. Collaboration, *Measurements of inclusive and differential Z boson production cross sections in* pp *collisions at $\sqrt{s} = 13$ TeV*, .

[3] **CMS** Collaboration, C. Collaboration, *Measurement of inclusive W and Z boson production cross sections in pp collisions at sqrt(s)=13 TeV*, .

[4] S. D. Drell and T.-M. Yan, *Massive Lepton Pair Production in Hadron-Hadron Collisions at High-Energies*, Phys. Rev. Lett. **25** (1970) 316–320. [Erratum: Phys. Rev. Lett.25,902(1970)].

[5] C. Anastasiou, C. Duhr, F. Dulat, E. Furlan, T. Gehrmann, F. Herzog, A. Lazopoulos, and B. Mistlberger, *High precision determination of the gluon fusion Higgs boson cross-section at the LHC*, JHEP **05** (2016) 058, [1602.00695].

[6] B. Mistlberger, *Higgs boson production at hadron colliders at N^{3}LO in QCD*, JHEP **05** (2018) 028, [1802.00833].

[7] A. Banfi, F. Caola, F. A. Dreyer, P. F. Monni, G. P. Salam, G. Zanderighi, and F. Dulat, *Jet-vetoed higgs cross section in gluon fusion at n3lo+nnll with small-r resummation*, *Journal of High Energy Physics* **2016** (2016), no. 4 49.

[8] C. Duhr, F. Dulat, and B. Mistlberger, *Higgs production in bottom-quark fusion to third order in the strong coupling*, 1904.09990.

[9] C. Duhr, F. Dulat, V. Hirschi, and B. Mistlberger, *Higgs production in bottom quark fusion: Matching the 4- and 5-flavour schemes to third order in the strong coupling*, 2004.04752.

[10] C. Duhr, F. Dulat, and B. Mistlberger, *The Drell-Yan cross section to third order in the strong coupling constant*, 2001.07717.

[11] X. Chen, T. Gehrmann, E. W. N. Glover, A. Huss, Y. Li, D. Neill, M. Schulze, I. W. Stewart, and H. X. Zhu, *Precise QCD Description of the Higgs Boson Transverse Momentum Spectrum*, *Phys. Lett.* **B788** (2019) 425–430, [1805.00736].

[12] F. Dulat, B. Mistlberger, and A. Pelloni, *Precision predictions at N^3LO for the Higgs boson rapidity distribution at the LHC*, *Phys. Rev.* **D99** (2019), no. 3 034004, [1810.09462].

[13] F. A. Dreyer and A. Karlberg, *Vector-Boson Fusion Higgs Pair Production at N^3LO*, *Phys. Rev.* **D98** (2018), no. 11 114016, [1811.07906].

[14] F. A. Dreyer and A. Karlberg, *Vector-Boson Fusion Higgs Production at Three Loops in QCD*, *Phys. Rev. Lett.* **117** (2016), no. 7 072001, [1606.00840].

[15] G. Altarelli, R. K. Ellis, and G. Martinelli, *Large Perturbative Corrections to the Drell-Yan Process in QCD*, *Nucl. Phys.* **B157** (1979) 461–497.

[16] J. Kubar-Andre and F. E. Paige, *Gluon Corrections to the Drell-Yan Model*, *Phys. Rev.* **D19** (1979) 221.

[17] K. Harada, T. Kaneko, and N. Sakai, *Hadronic Lepton Pair Production Beyond the Leading Order in Perturbative QCD*, *Nucl. Phys.* **B155** (1979) 169–188. [Erratum: Nucl. Phys.B165,545(1980)].

[18] P. Aurenche and J. Lindfors, *QCD Corrections to Direct Lepton Production in Hadronic Collisions*, *Nucl. Phys.* **B185** (1981) 274–300.

[19] R. Hamberg, W. L. van Neerven, and T. Matsuura, *A complete calculation of the order $\alpha - s^2$ correction to the Drell-Yan K factor*, *Nucl. Phys.* **B359** (1991) 343–405. [Erratum: Nucl. Phys.B644,403(2002)].

[20] C. Anastasiou, L. J. Dixon, K. Melnikov, and F. Petriello, *High precision QCD at hadron colliders: Electroweak gauge boson rapidity distributions at NNLO*, *Phys. Rev.* **D69** (2004) 094008, [hep-ph/0312266].

[21] K. Melnikov and F. Petriello, *The W boson production cross section at the LHC through $O(\alpha_s^2)$*, *Phys. Rev. Lett.* **96** (2006) 231803, [hep-ph/0603182].

[22] R. V. Harlander and W. B. Kilgore, *Next-to-next-to-leading order Higgs production at hadron colliders*, *Phys. Rev. Lett.* **88** (2002) 201801, [hep-ph/0201206].

[23] C. Anastasiou, C. Duhr, F. Dulat, F. Herzog, and B. Mistlberger, *Higgs Boson Gluon-Fusion Production in QCD at Three Loops*, *Phys. Rev. Lett.* **114** (2015) 212001, [1503.06056].

[24] C. Anastasiou and K. Melnikov, *Higgs boson production at hadron colliders in NNLO QCD*, *Nuclear Physics B* **646** (dec, 2002) 220–256, [0207004].

[25] C. Anastasiou and K. Melnikov, *Pseudoscalar Higgs boson production at hadron colliders in next-to-next-to-leading order QCD*, *Physical Review D* **67** (feb, 2003) 037501.

[26] C. Anastasiou, L. Dixon, and K. Melnikov, *NLO Higgs boson rapidity distributions at hadron colliders*, *Nuclear Physics B - Proceedings Supplements* **116** (mar, 2003) 193–197.

[27] C. Anastasiou, L. Dixon, K. Melnikov, and F. Petriello, *Dilepton Rapidity Distribution in the Drell-Yan Process at Next-to-Next-to-Leading Order in QCD*, *Physical Review Letters* **91** (oct, 2003) 182002.

[28] C. Anastasiou, L. Dixon, K. Melnikov, and F. Petriello, *High-precision QCD at hadron colliders: Electroweak gauge boson rapidity distributions at next-to-next-to leading order*, *Physical Review D* **69** (may, 2004) 094008.

[29] F. Tkachov, *A theorem on analytical calculability of 4-loop renormalization group functions*, *Physics Letters B* **100** (mar, 1981) 65–68.

[30] K. Chetyrkin and F. Tkachov, *Integration by parts: The algorithm to calculate β-functions in 4 loops*, *Nuclear Physics B* **192** (nov, 1981) 159–204.

[31] S. Laporta, *High precision calculation of multiloop Feynman integrals by difference equations*, *Int. J. Mod. Phys.* **A15** (2000) 5087–5159, [`hep-ph/0102033`].

[32] A. V. Kotikov, *Differential equations method: New technique for massive Feynman diagrams calculation*, *Phys. Lett.* **B254** (1991) 158–164.

[33] A. V. Kotikov, *Differential equations method: The Calculation of vertex type Feynman diagrams*, *Phys. Lett.* **B259** (1991) 314–322.

[34] A. V. Kotikov, *Differential equation method: The Calculation of N point Feynman diagrams*, *Phys. Lett.* **B267** (1991) 123–127.

[35] J. M. Henn, *Multiloop integrals in dimensional regularization made simple*, *Phys. Rev. Lett.* **110** (2013) 251601, [`1304.1806`].

[36] T. Gehrmann and E. Remiddi, *Differential equations for two loop four point functions*, *Nucl. Phys.* **B580** (2000) 485–518, [`hep-ph/9912329`].

[37] T. Gehrmann, G. Heinrich, T. Huber, and C. Studerus, *Master integrals for massless three-loop form-factors: One-loop and two-loop insertions*, *Phys. Lett.* **B640** (2006) 252–259, [`hep-ph/0607185`].

[38] G. Heinrich, T. Huber, and D. Maitre, *Master integrals for fermionic contributions to massless three-loop form-factors*, *Phys. Lett.* **B662** (2008) 344–352, [`0711.3590`].

[39] G. Heinrich, T. Huber, D. A. Kosower, and V. A. Smirnov, *Nine-Propagator Master Integrals for Massless Three-Loop Form Factors*, *Phys. Lett.* **B678** (2009) 359–366, [`0902.3512`].

[40] R. N. Lee, A. V. Smirnov, and V. A. Smirnov, *Analytic Results for Massless Three-Loop Form Factors*, *JHEP* **04** (2010) 020, [`1001.2887`].

[41] P. A. Baikov, K. G. Chetyrkin, A. V. Smirnov, V. A. Smirnov, and M. Steinhauser, *Quark and gluon form factors to three loops*, *Phys. Rev. Lett.* **102** (2009) 212002, [`0902.3519`].

[42] T. Gehrmann, E. W. N. Glover, T. Huber, N. Ikizlerli, and C. Studerus, *Calculation of the quark and gluon form factors to three loops in QCD*, *JHEP* **06** (2010) 094, [`1004.3653`].

[43] T. Gehrmann, E. W. N. Glover, T. Huber, N. Ikizlerli, and C. Studerus, *The quark and gluon form factors to three loops in QCD through to $O(\epsilon^2)$*, *JHEP* **11** (2010) 102, [1010.4478].

[44] C. Anastasiou, C. Duhr, F. Dulat, F. Herzog, and B. Mistlberger, *Real-virtual contributions to the inclusive Higgs cross-section at N^3LO*, *JHEP* **12** (2013) 088, [1311.1425].

[45] W. B. Kilgore, *One-loop single-real-emission contributions to $pp \to H + X$ at next-to-next-to-next-to-leading order*, *Phys. Rev.* **D89** (2014), no. 7 073008, [1312.1296].

[46] C. Duhr and T. Gehrmann, *The two-loop soft current in dimensional regularization*, *Phys. Lett.* **B727** (2013) 452–455, [1309.4393].

[47] Y. Li and H. X. Zhu, *Single soft gluon emission at two loops*, *JHEP* **11** (2013) 080, [1309.4391].

[48] F. Dulat and B. Mistlberger, *Real-Virtual-Virtual contributions to the inclusive Higgs cross section at N3LO*, 1411.3586.

[49] T. Ahmed, M. Mahakhud, P. Mathews, N. Rana, and V. Ravindran, *Two-loop QCD corrections to Higgs $\to b + \bar{b} + g$ amplitude*, *JHEP* **08** (2014) 075, [1405.2324].

[50] C. Anastasiou, C. Duhr, F. Dulat, E. Furlan, T. Gehrmann, F. Herzog, and B. Mistlberger, *Higgs boson gluon–fusion production at threshold in N^3LO QCD*, *Phys. Lett.* **B737** (2014) 325–328, [1403.4616].

[51] Y. Li, A. von Manteuffel, R. M. Schabinger, and H. X. Zhu, *N^3LO Higgs boson and Drell-Yan production at threshold: The one-loop two-emission contribution*, *Phys. Rev.* **D90** (2014), no. 5 053006, [1404.5839].

[52] Y. Li, A. von Manteuffel, R. M. Schabinger, and H. X. Zhu, *Soft-virtual corrections to Higgs production at N^3LO*, *Phys. Rev.* **D91** (2015) 036008, [1412.2771].

[53] C. Anastasiou, C. Duhr, F. Dulat, E. Furlan, F. Herzog, and B. Mistlberger, *Soft expansion of double-real-virtual corrections to Higgs production at N^3LO*, *JHEP* **08** (2015) 051, [1505.04110].

[54] C. Anastasiou, C. Duhr, F. Dulat, and B. Mistlberger, *Soft triple-real radiation for Higgs production at N3LO*, *JHEP* **07** (2013) 003, [1302.4379].

[55] O. V. Tarasov, A. A. Vladimirov, and A. Yu. Zharkov, *The Gell-Mann-Low Function of QCD in the Three Loop Approximation*, *Phys. Lett.* **93B** (1980) 429–432.

[56] S. A. Larin and J. A. M. Vermaseren, *The Three loop QCD Beta function and anomalous dimensions*, *Phys. Lett.* **B303** (1993) 334–336, [hep-ph/9302208].

[57] T. van Ritbergen, J. A. M. Vermaseren, and S. A. Larin, *The Four loop beta function in quantum chromodynamics*, *Phys. Lett.* **B400** (1997) 379–384, [hep-ph/9701390].

[58] P. A. Baikov, K. G. Chetyrkin, and J. H. Kühn, *Five-Loop Running of the QCD coupling constant*, *Phys. Rev. Lett.* **118** (2017), no. 8 082002, [1606.08659].

[59] F. Herzog, B. Ruijl, T. Ueda, J. A. M. Vermaseren, and A. Vogt, *The five-loop beta function of Yang-Mills theory with fermions*, *JHEP* **02** (2017) 090, [1701.01404].

[60] S. Buehler and A. Lazopoulos, *Scale dependence and collinear subtraction terms for Higgs production in gluon fusion at N3LO*, *JHEP* **10** (2013) 096, [1306.2223].

[61] M. Höschele, J. Hoff, A. Pak, M. Steinhauser, and T. Ueda, *Higgs boson production at the LHC: NNLO partonic cross sections through order ϵ and convolutions with splitting functions to N^3LO, Phys. Lett.* **B721** (2013) 244–251, [1211.6559].

[62] M. Höschele, J. Hoff, A. Pak, M. Steinhauser, and T. Ueda, *MT: A Mathematica package to compute convolutions, Comput. Phys. Commun.* **185** (2014) 528–539, [1307.6925].

[63] S. Moch, J. A. M. Vermaseren, and A. Vogt, *The Three loop splitting functions in QCD: The Nonsinglet case, Nucl. Phys.* **B688** (2004) 101–134, [hep-ph/0403192].

[64] A. Vogt, S. Moch, and J. A. M. Vermaseren, *The Three-loop splitting functions in QCD: The Singlet case, Nucl. Phys.* **B691** (2004) 129–181, [hep-ph/0404111].

[65] J. Ablinger, A. Behring, J. Blmlein, A. De Freitas, A. von Manteuffel, and C. Schneider, *The three-loop splitting functions $P_{qg}^{(2)}$ and $P_{gg}^{(2,N_F)}$, Nucl. Phys.* **B922** (2017) 1–40, [1705.01508].

[66] C. Duhr and F. Dulat, *PolyLogTools — polylogs for the masses, JHEP* **08** (2019) 135, [1904.07279].

[67] E. Remiddi and J. A. M. Vermaseren, *Harmonic polylogarithms, Int. J. Mod. Phys.* **A15** (2000) 725–754, [hep-ph/9905237].

[68] A. B. Goncharov, *Multiple polylogarithms, cyclotomy and modular complexes, Mathematical Research Letters* **5** (1998), no. 4 497–516.

[69] V. N. Gribov and L. N. Lipatov, *Deep inelastic e p scattering in perturbation theory, Sov. J. Nucl. Phys.* **15** (1972) 438–450. [Yad. Fiz.15,781(1972)].

[70] G. Altarelli and G. Parisi, *Asymptotic Freedom in Parton Language, Nucl. Phys.* **B126** (1977) 298–318.

[71] Y. L. Dokshitzer, *Calculation of the Structure Functions for Deep Inelastic Scattering and e+ e- Annihilation by Perturbation Theory in Quantum Chromodynamics., Sov. Phys. JETP* **46** (1977) 641–653. [Zh. Eksp. Teor. Fiz.73,1216(1977)].

[72] T. O. Eynck, E. Laenen, and L. Magnea, *Exponentiation of the Drell-Yan cross-section near partonic threshold in the DIS and MS-bar schemes, JHEP* **06** (2003) 057, [hep-ph/0305179].

[73] S. Moch and A. Vogt, *Higher-order soft corrections to lepton pair and Higgs boson production, Phys. Lett.* **B631** (2005) 48–57, [hep-ph/0508265].

[74] T. Ahmed, M. Mahakhud, N. Rana, and V. Ravindran, *Drell-Yan Production at Threshold to Third Order in QCD, Phys. Rev. Lett.* **113** (2014), no. 11 112002, [1404.0366].

[75] S. Catani, L. Cieri, D. de Florian, G. Ferrera, and M. Grazzini, *Threshold resummation at N^3LL accuracy and soft-virtual cross sections at N^3LO, Nucl. Phys.* **B888** (2014) 75–91, [1405.4827].

[76] A. A.H., G. Das, M. Kumar, P. Mukherjee, V. Ravindran, and K. Samanta, *Resummed Drell-Yan cross-section at N^3LL*, 2001.11377.

[77] S. Moch and A. Vogt, *On non-singlet physical evolution kernels and large-x coefficient functions in perturbative QCD, JHEP* **11** (2009) 099, [0909.2124].

[78] G. Soar, S. Moch, J. A. M. Vermaseren, and A. Vogt, *On Higgs-exchange DIS, physical evolution kernels and fourth-order splitting functions at large x, Nucl. Phys.* **B832** (2010) 152–227, [0912.0369].

[79] D. de Florian, J. Mazzitelli, S. Moch, and A. Vogt, *Approximate N^3LO Higgs-boson production cross section using physical-kernel constraints*, JHEP **10** (2014) 176, [1408.6277].

[80] S. Marzani, *High Energy Resummation in Quantum Chromo-Dynamics.* PhD thesis, University of Edinburgh, 2008.

[81] S. Marzani and R. D. Ball, *High Energy Resummation of Drell-Yan Processes*, Nucl. Phys. **B814** (2009) 246–264, [0812.3602].

[82] C.-H. Kom and W. Stirling, *Charge asymmetry in W + jets production at the LHC*, Eur. Phys. J. C **69** (2010) 67–73, [1004.3404].

[83] **Particle Data Group** Collaboration, M. Tanabashi *et al.*, *Review of Particle Physics*, Phys. Rev. **D98** (2018), no. 3 030001.

[84] J. Butterworth *et al.*, *PDF4LHC recommendations for LHC Run II*, J. Phys. **G43** (2016) 023001, [1510.03865].

[85] M. Cacciari and N. Houdeau, *Meaningful characterisation of perturbative theoretical uncertainties*, JHEP **09** (2011) 039, [1105.5152].

[86] M. Bonvini, *Probabilistic definition of the perturbative theoretical uncertainty from missing higher orders*, 2006.16293.

[87] **NNPDF** Collaboration, R. D. Ball *et al.*, *Parton distributions from high-precision collider data*, Eur. Phys. J. **C77** (2017), no. 10 663, [1706.00428].

[88] G. Balossini, G. Montagna, C. M. Carloni Calame, M. Moretti, O. Nicrosini, F. Piccinini, M. Treccani, and A. Vicini, *Combination of electroweak and QCD corrections to single W production at the Fermilab Tevatron and the CERN LHC*, JHEP **01** (2010) 013, [0907.0276].

[89] A. Denner, S. Dittmaier, T. Kasprzik, and A. Muck, *Electroweak corrections to W + jet hadroproduction including leptonic W-boson decays*, JHEP **08** (2009) 075, [0906.1656].

[90] A. Denner, S. Dittmaier, T. Kasprzik, and A. Mck, *Electroweak corrections to monojet production at the LHC*, Eur. Phys. J. **C73** (2013), no. 2 2297, [1211.5078].

[91] D. Kara, *Corrections of Order $\alpha\alpha_s$ to W Boson Decays*, Nucl. Phys. **B877** (2013) 683–718, [1307.7190].

[92] W. B. Kilgore and C. Sturm, *Two-Loop Virtual Corrections to Drell-Yan Production at order $\alpha_s\alpha^3$*, Phys. Rev. **D85** (2012) 033005, [1107.4798].

[93] A. Kotikov, J. H. Kuhn, and O. Veretin, *Two-Loop Formfactors in Theories with Mass Gap and Z-Boson Production*, Nucl. Phys. **B788** (2008) 47–62, [hep-ph/0703013].

[94] S. Dittmaier, A. Huss, and C. Schwinn, *Mixed QCD-electroweak $O(\alpha_s\alpha)$ corrections to Drell-Yan processes in the resonance region: pole approximation and non-factorizable corrections*, Nucl. Phys. **B885** (2014) 318–372, [1403.3216].

[95] F. Buccioni, F. Caola, M. Delto, M. Jaquier, K. Melnikov, and R. Röntsch, *Mixed QCD-electroweak corrections to on-shell Z production at the LHC*, 2005.10221.

[96] M. Delto, M. Jaquier, K. Melnikov, and R. Röntsch, *Mixed QCD⊗QED corrections to on-shell Z boson production at the LHC*, JHEP **01** (2020) 043, [1909.08428].

[97] R. Bonciani, F. Buccioni, N. Rana, I. Triscari, and A. Vicini, *NNLO QCD×EW corrections to Z production in the q$\bar{q}$ channel*, Phys. Rev. **D101** (2020), no. 3 031301, [1911.06200].

[98] R. Bonciani, F. Buccioni, N. Rana, and A. Vicini, *NNLO QCD×EW corrections to on-shell Z production*, [2007.06518](https://arxiv.org/abs/2007.06518).

[99] F. Dulat, B. Mistlberger, and A. Pelloni, *Differential Higgs production at N^3LO beyond threshold*, *JHEP* **01** (2018) 145, [[1710.03016](https://arxiv.org/abs/1710.03016)].

[100] L. Cieri, X. Chen, T. Gehrmann, E. N. Glover, and A. Huss, *Higgs boson production at the LHC using the q_T subtraction formalism at N^3LO QCD*, *JHEP* **02** (2019) 096, [[1807.11501](https://arxiv.org/abs/1807.11501)].

[101] G. Billis, M. A. Ebert, J. K. Michel, and F. J. Tackmann, *A Toolbox for q_T and 0-Jettiness Subtractions at N^3LO*, [1909.00811](https://arxiv.org/abs/1909.00811).